Molecular Neurobiology (2019) 56:2057–2072
https://doi.org/10.1007/s12035-018-1196-4

Expression of the Cerebral Olfactory Receptors Olfr110/111 and Olfr544 Is Altered During Aging and in Alzheimer's Disease-Like Mice

Fanny Gaudel[1] · Delphine Stephan[1] · Véréna Landel[1] · Gilles Sicard[1] · François Féron[1] · Gaëlle Guiraudie-Capraz[1]

Received: 18 January 2018 / Accepted: 26 June 2018 / Published online: 8 July 2018

Abstract

A growing number of studies report the expression of olfactory receptors (ORs) in many non-chemosensory tissues and organs. However, within the brain, very few ectopic ORs are exhaustively documented. Their kinetic expression, cellular localization, and functions remain elusive. Using cDNA microarrays, quantitative PCR, and immunohistochemistry, we studied the cellular and sub-cellular localization of Olfr110/111 and Olfr544 and their timely expression in various brain areas of wild-type and transgenic Alzheimer's disease-like (5xFAD) mice. We observed that Olfr110/111 and Olfr544 proteins are mainly expressed by neurons in cortical and hippocampal regions and, to a lesser extent, by astrocytes, microglia, oligodendrocytes, and endothelial cells. In addition, both ORs are present at the cell membrane and co-expressed with the olfactory Gαolf protein, suggesting that they can be functional. Remarkably, we also found that the expression of the mRNA encoding for Olfr110/111 tends to increase with age in both the cortex and hippocampus of wild-type and transgenic mice. Moreover, *Olfr110/111* transcript expression is markedly impaired in the brain of Alzheimer's disease-like mice. A different profile is noticed for *Olfr544*, for which an overexpression is observed only in the cortex of 9-month-old animals. In addition, in transgenic mice, olfactory receptors are observed near amyloid plaques. Altogether, our findings indicate that ORs may play a role in brain functioning, in normal and pathological conditions.

Keywords Olfactory receptors · Alzheimer's disease · Neurons · Aging · Hippocampus · Cortex

Introduction

At the time of their very first identification, nasal olfactory receptors (OR) were described as "seven transmembrane domain proteins whose expression is restricted to the olfactory epithelium" [1]. However, during the following decade, "ectopic" ORs were reported to be expressed in rodent and human non-chemosensory tissues and organs, including testis [2–12], spermatozoa midpiece and flagella [13, 14], lung [15–17], skin [18–20], kidney [6, 21, 22], pancreas [23], and a variety of other body parts [24–27]. The presence of such receptors in non-olfactory tissues prompted a vivid interest, and numerous studies focused on the elucidation of their roles in major cellular functions. For example, it has been demonstrated that ORs are involved in glucose homeostasis [23], keratinocyte proliferation and migration [18], detection of irritants in pulmonary neuroendocrine cells [16], myocyte adhesion and migration [28], melanogenesis [19], gut motility [29], renal secretion of renin [30], and spermatozoa motility [31]. In the central nervous system, PCR, microarray, and next-generation sequencing studies revealed the expression of numerous genes encoding for human, rat, and mouse ORs [32–38]. At the protein level, three human ORs (OR2A4, OR2H2, and OR6K3) were immunodetected in the cortex and the hippocampus, along with two of their olfactory signaling partners, Gαolf and adenylyl cyclase 3 (AC3) [37]. Moreover, a dysregulated expression of human ORs and olfactory-related genes was observed in several pathologies, such as Alzheimer's disease, Creutzfeldt-Jakob's disease, progressive supranuclear palsy, schizophrenia, and Parkinson's disease [36, 37, 39]. With regard to the latter, it has been shown for example that several OR transcripts were expressed in murine mesencephalic dopaminergic neurons [38].

François Féron and Gaëlle Guiraudie-Capraz equally supervised this work.

Electronic supplementary material The online version of this article (https://doi.org/10.1007/s12035-018-1196-4) contains supplementary material, which is available to authorized users.

✉ Gaëlle Guiraudie-Capraz
gaelle.guiraudie@univ-amu.fr

[1] Aix Marseille Univ, CNRS, INP, Marseille, France

Significant progress has been made in clarifying the roles of ORs in some non-olfactory tissues. However, next to nothing is known about the physiological functions of ORs within the nervous system. For the current study, we decided to start at square 0 and assess the kinetic cerebral expression and subcellular localization of two olfactory receptors—*Olfr110/111* and *Olfr544*—and partners, during aging and in a mouse model of Alzheimer's disease. These two ORs were selected for the following reasons. On the one hand, the transcript *Olfr110* is overexpressed in the brain of a transgenic Alzheimer's disease mouse model (APP/PS1) and co-expressed with *Gαolf* and *AC3* [36]. On the other hand, we observed that the transcript *Olfr544* is overexpressed in the cortex and hippocampus of transgenic 9-month-old 5xFAD mice, another animal model of Alzheimer's disease (Supplementary Table 1). *Olfr110/111* human ortholog is *OR5V1*, a class II OR. No conserved *Olfr544* has been identified in humans. However, according to the Allen Brain Atlas [40], *OR52K2*, one of the most expressed OR transcript in the human brain, *OR52K2*, shares 37% identity with *Olfr544*. In addition, specific and reliable antibodies are available for Olfr110/111 and Olfr544 corresponding proteins.

For our purpose, we used cellular and molecular tools such as cDNA microarrays, polymerase chain reaction, and immunohistochemistry on various tissues and brain areas from wild-type (WT) and Alzheimer's-like (5xFAD model) mice, at various ages. We observed that *Olfr110/111* and *Olfr544* are expressed within both the cortex and hippocampus of WT and 5xFAD transgenic mice, at the transcriptional and protein levels. In these structures, transcripts of both ORs display age- and pathology-associated variations of expression. At the cellular level, Olfr110/111 and Olfr544 proteins are expressed at the membrane of neurons and several other cell types, in combination with Gαolf.

Materials and Methods

Animals

This study was performed using 5xFAD transgenic mice, overexpressing two transgenes bearing five mutations linked to familial Alzheimer's disease: human *APP* (Swedish mutation K670N, M671L; Florida mutation I716V; London mutation V717I) and human *Presenilin 1* (PSEN1 M146L, L286V), under the transcriptional control of the mouse *Thy1* promoter. The 5xFAD lines from the C57Bl/6 genetic background were maintained by crossing heterozygous transgenic mice with C57Bl/6 F1 breeders. These mice exhibit Alzheimer's disease-related symptoms earlier than other animal models, and amyloid deposition starts in the cortex and subiculum at 2 months of age [41]. Heterozygous male 5xFAD transgenic animals and wild-type controls were obtained after breeding of progenitors purchased from the Jackson Laboratory. Genotyping was performed by PCR analysis of tail DNA in order to detect the human *APP* gene. The animals were housed in a temperature-controlled environment (22 ± 2 °C) with a light/dark cycle of 12 h. The animals had ad libitum access to drinking water and standard food pellets. Animal manipulations were carried out in accordance with the guidelines published in the European Communities Council Directive of November 24, 1986 (86/609/EEC). All efforts were made to reduce animal stress, suffering, and numbers.

Gene Expression Profiling Using Microarray Procedure

Cortical and hippocampal RNA samples from three WT and three 5xFAD mice, aged 1, 4, 6, and 9 months (M1, M4, M6, and M9), were pooled for microarray hybridization. Sample amplification, labeling, and hybridization were performed in line with the Agilent one-color microarray-base analysis (Low Input Quick Amp labeling) protocol (Agilent Technologies, Les Ulis, France). Briefly, total RNA was reverse-transcribed into cDNA using the *T7* promoter primer. The reaction intending to synthesize cyanine-3-labeled cRNA from cDNA was performed in a solution containing dNTP mix, T7 RNA polymerase, and cyanine 3-dCTP and then incubated at 40 °C for 2 h. Labeled cRNA was purified and fragmented before hybridization on Agilent 8x60k Mouse Gene Expression Arrays (Agilent Technologies), containing 62,975 oligonucleotide probes, at 65 °C for 17 h. Raw microarray signals were scanned and extracted using Agilent Feature Extraction Software (Agilent Technologies). AgiND R package was used for quality control and normalization. Quantile methods and a background correction were applied for data normalization. Microarray data are available in the ArrayExpress database under accession number E-MTAB-1937.

RNA Purification and Quantitative Real-Time PCR

Cortex, hippocampus, cerebellum, olfactory mucosa, and eyes were collected from WT and 5xFAD transgenic mice aged M4, M6, M9, and M12 ($n = 6$ per group). Total RNA was isolated using RNeasy Mini Kit (Qiagen, Courtaboeuf, France), according to the manufacturer's instructions.

Total RNA was reverse transcribed with the High-Capacity RNA-to-cDNA Kit (Applied Biosystems, Thermo Fisher Scientific, Villebon sur Yvette, France) following the manufacturer's instructions and using a Veriti™ 96-Well thermal cycler (Applied Biosystems). Real-time quantitative PCRs were carried out (Applied Biosystems® 7500 Fast, Life Technologies) to detect the expression of the two molecular targets of interest using a combination of specific primers for

Olfr110/111 and *Olfr544*. *GAPDH* was chosen as a housekeeping gene and its expression levels served as reference. The real-time PCR reactions were carried out with 50 ng of cDNA in a mix solution containing 1× iTaq™ Universal SYBR® Green Supermix (Bio-Rad, Kidlington, UK) and 300 nM of forward and reverse primers. Oligonucleotides were designed from the nucleotide sequences described in GenBank:

Olfr110/111 forward primer: 5′-ACCACCTGAATGAA TTGCAGTAT-3′
Olfr110/111 reverse primer: 5′-CAGCTATGGTCACC ACAATGAT-3′
Olfr544 forward primer: 5′-GGACATCTCGCTGA ATAAGACG-3′
Olfr544 reverse primer: 5′-CCAGGACTCGGTTG AAGATG-3′
GAPDH forward primer: 5′-TGACGTGCCGCCTG GAGAAA-3′
GAPDH reverse primer: 5′-AGTGTAGCCCAAGA TGCCCTTCAG-3′

Samples were amplified in triplicates. Mean Ct for each sample was calculated, and relative expression levels were determined according to the ΔΔCt method: ΔCt values represent the normalized levels of each target gene compared to the *GAPDH* control, and ΔΔCt values were calculated by subtracting the mean ΔCt of the control population to the sample ΔCt. Relative expression levels were calculated using the $2^{-\Delta\Delta Ct}$ equation. Negative fold change values were obtained by the equation 1/(mean $2^{-\Delta\Delta Ct}$) of each group.

OR Construct, Cloning, and Expression in HEK Cells

The 317 amino acid sequence of Olfr110 and the 334 amino acid sequence of Olfr544 were obtained from the online NCBI Protein database (#AAP71232.1 and #ALI87966.1, respectively). To facilitate protein expression and purification from mammalian cells, the following insertions were performed: (1) a Kozak sequence (GCCACCATGG), immediately before the start codon; (2) a Flag epitope tag (DYKDDDDK) at the N-terminus of both genes after the start codon; and (3) the bovine rhodopsin C9 (rho1D4) epitope tag (TETSQVAPA) at the C-terminus of the protein. Two glycine linkers (GG) were inserted after the Flag epitope and before the rho1D4 epitope, respectively, as described by Belloir et al. [42]. *Olfr110* and *Olfr544* genes were cloned into the pcDNA3.1 expression vector (Life Technologies, ThermoFisher Scientific, France) to produce the pcDNA3.1-FLAG-Olfr110-rho1D4 vector and pcDNA3.1-FLAG-Olfr544-rho1D4 vector. The native genes coding for Olfr110 and Olfr544 were also cloned in pcDNA3.1 vector to produce pcDNA3.1-Olfr110 and pcDNA3.1-Olfr544 vectors. The plasmids were amplified in *E. coli* TOP10 cells (Life Technologies, ThermoFisher Scientific, France) and purified with a QIAfilter Plasmid Midi kit (Qiagen, Courtaboeuf, France).

The human HEK293T cells (HEK293T) were grown in DMEM Glutamax culture medium, supplemented with 10% fetal bovine serum, non-essential amino acids (0.1 mM), penicillin (100 units/mL), and streptomycin (100 mg/mL) (Life Technologies, ThermoFisher Scientific, France). The cells were cultivated at 37 °C in a humidified atmosphere containing 5% CO_2. The pcDNA3.1-Flag-Olfr110-rho1D4 and the pcDNA3.1-Flag-Olfr544-rho1D4 plasmids were transfected into cells using Fugene HD (Promega, Charbonnieres Les Bains, France). After 24–48 h, the cells were collected.

Immunocytochemistry and Western Blot

OR-transfected HEK293T cells were seeded onto 22-mm coverslips. Transiently transfected cells were washed with PBS 1×, fixed with 4% paraformaldehyde (Antigenfix solution, Diapath, MM France, Brignais, France), and then incubated with mouse anti-Flag antibody (F3165, 1:500, Sigma, France) and rabbit anti-OR antibodies (Olfr110: ab177327, 1:100, Abcam, France, and Olfr544: OSR00035G, 1:200, Invitrogen, France) diluted in PBS with 0.1% Tween 20, 3% BSA, and 2.25% glycine (Sigma, France), for 1 h at room temperature. Primary antibodies were detected with goat anti-mouse Alexa Fluor 488 (A11029, 1:500, Life Technologies) for Flag and goat anti-rabbit Alexa Fluor 594 (A11037, 1:500, Life Technologies, ThermoFisher Scientific, France) for ORs, all diluted in PBS containing 1% Tween 20, 3% BSA, and 2.25% glycine, for 1 h at room temperature in the dark. After washing, the coverslips were inverted and mounted on glass slides with Prolong Gold Antifade reagent (Life Technologies). Images were obtained using a LSM 700 (Zeiss, Jena, Germany) confocal microscope, and images were analyzed using ImageJ (NIH) software.

For the Western blot analysis, lysates of HEK-transfected cells (HEK-110, HEK-544, and HEK-pcDNA3.1) were prepared by incubating cells on ice for 30 min in a RIPA buffer supplemented with 1% protease inhibitor cocktail (Sigma, France). Protein concentration was quantified by using the Bio-Rad *DC*™ protein assay kit according to the manufacturer's instructions (Bio-Rad). Equal amounts of proteins were separated on 12% SDS-PAGE and transferred to nitrocellulose membranes (GE Healthcare, Dutscher, Brumath, France). After blocking, membranes were probed with the following antibodies: polyclonal anti-Olfr110 (ab177327, 1:100, Abcam, France) and polyclonal anti-Olfr544 (OSR00035G, 1:200, Invitrogen, France). Membranes were then incubated with the appropriate horseradish peroxidase-conjugated secondary IgG antibodies (Jackson Immunoresearch, West Grove, PA, USA). Immunoblot signals were visualized with ECL chemiluminescence kit (GE Healthcare).

Perfusion and Immunohistochemistry

WT and transgenic 5xFAD mice at M6 and M9 ($n = 3$ per group) were deeply anesthetized with an intraperitoneal injection of sodium pentobarbital (355 mg/kg, Ceva Santé Animal, Libourne, France) and perfused transcardially with 0.9% saline, followed by 4% paraformaldehyde (Antigenfix solution, Diapath, MM France, Brignais, France). Brains removed from perfused mice and heads from newborn mice P5 were post-fixed overnight in the 4% paraformaldehyde fixative solution and then cryoprotected in 30% sucrose in phosphate buffer saline (PBS) solution. Brains and noses were cryosectioned to 16-μm slices in hippocampal, cerebellar areas, and olfactory epithelium (OE) using a Leica CM3050S cryostat (Leica Microsystems, Nanterre, France), and stored at − 80 °C until immunostaining.

Brain and OE sections were gently unfrozen at room temperature, and antigen retrieval was carried out by immersion in sodium citrate buffer (10 mM sodium citrate, 0.05% Tween-20, pH 6.0) for 20 min at 75 °C and then progressively cooled down for 15 min. After a washing step in 0.05% PBS-Tween 20, sections were blocked for 1 h at room temperature in a blocking buffer containing 0.3% Triton X-100, 3% bovine albumin serum (BSA), 10% PBS 10×, and 5% normal goat or donkey serum (Jackson Immunoresearch Laboratories, West Grove, PA, USA).

For co-immunostaining, titration experiments were performed at the following dilutions 1:100, 1:200, 1:300, 1:500, and 1:1000. Final experiments were carried on sections using the primary antibodies raised against Olfr110/111 (ab177327, 1:100, Abcam, France) or Olfr544 (OSR00035G, 1:200, Invitrogen, France) and either: anti-NeuN (ab104224, 1:500, Abcam) for neuronal staining, or anti-GFAP (MAB360, 1:500, Millipore, Merck Chimie, Fontenay sous Bois, France) for astrocytes staining, or anti-MBP (MCA409S, 1:200, Bio-Rad) for oligodendrocytes staining, or Collagen IV (C7510-50H, 1:1000, US Biological, Salem, MA, USA) for endothelial cells staining, or anti-6E10 (SIG-39320, 1:300, Covance, Ozyme, Saint-Quentin, France) for amyloid plaques staining, diluted in the blocking solution for 2 h at room temperature. After washing in PBS, sections were incubated with secondary antibodies, respectively, goat anti-rabbit Alexa Fluor 594 (A11037, 1:500, Life Technologies, ThermoFisher Scientific, France) to immunodetect Olfr antigens, and either goat anti-mouse Alexa Fluor 488 (A11029, 1:500, Life Technologies) for NeuN, GFAP, and 6E10, or goat anti-rat Alexa Fluor 488 (A11006, 1:500, Life Technologies) for MBP, or donkey anti-goat Alexa Fluor 488 (A11055, 1:1000, Life Technologies) for collagen IV for 1.5 h at room temperature. Nuclei were stained using DNA intercalant Hoechst (H6024, 1:1000, Sigma-Aldrich, Merck, Saint-Quentin Fallavier, France).

For co-immunostaining of ORs with either Iba1 or Gαolf protein, sections were first incubated with the primary antibodies raised against Olfr110/111 or Olfr544 overnight at 4 °C. After washing in PBS, sections were incubated for 1.5 h with goat anti-rabbit Alexa Fluor 594 at room temperature, followed by a blocking step, 2 h incubation at room temperature with 5% normal rabbit serum (Jackson Immunoresearch Laboratories) in PBS. After an additional 2-h incubation with AffiniPure Fab Goat anti-Rabbit fragments (Jackson Immunoresearch Laboratories) in PBS at room temperature, sections were incubated with the primary antibodies raised against Iba1 (019–19,741, 1:1500, Wako, Sobioda, Montbonnot-Saint-Martin, France) or Gαolf (PA5–27964, 1:1000, Thermo Fisher Scientific) overnight at 4 °C, and with the corresponding secondary antibody goat anti-rabbit Alexa Fluor 488 for 1.5 h at room temperature. Nuclei were stained with DNA intercalant Hoechst.

Co-staining of sections with Alexa Fluor 488-conjugated Wheat Germ Agglutinin (WGA-Alexa, 3 μg/ml, Molecular Probes) was used for visualization of the cell membrane. After washing with HBSS, incubation for 10 min with 3 μg/ml of WGA Alexa Fluor 488 conjugate in HBSS and a blocking step for 1 h at room temperature, sections were incubated for 2 h at room temperature with Olfr110/111 or Olfr544 antibodies. Sections were then incubated for 1.5 h with the corresponding secondary antibody goat anti-rabbit Alexa Fluor 594 and DNA intercalant Hoechst.

Sections were mounted using Prolong Gold Antifade reagent (Life Technologies). Negative control immunostaining was performed without the primary antibody, and no immunoreactivity was confirmed. Sections were observed under a LSM 700 (Zeiss, Jena, Germany) confocal microscope, and images were analyzed using ImageJ (NIH) software.

Statistics

Statistical analyses were performed with the unpaired, two-tailed Mann-Whitney non-parametric statistical test. All data are presented as means ± SEM and were analyzed using GraphPad Prism 6 software. Quantitative PCR data were normalized with M4 animals $2^{-\Delta\Delta Ct}$ values fixed to 1, and the negative fold change values were obtained by the equation $1/(\text{mean } 2^{-\Delta\Delta Ct})$ of each group. Differences between mean values were considered statistically significant when $p < 0.05$ (*) and $p < 0.01$ (**).

Results

AD Progression Induces a Massive Time- and Area-Related Dysregulation of OR Expression

The cortex and hippocampus of 5xFAD mice display an extensive dysregulated expression of transcripts coding for olfactory receptors. Most of them are misexpressed at only one

time point, whatever the tissue considered. Out of the 164 dysregulated OR transcripts, only ten—*Olfr446*, *Olfr538*, *Olfr544*, *Olfr574*, *Olfr720*, *Olfr868*, *Olfr1133*, *Olfr1335*, *Olfr1466*, and *Olfr1500*—are misexpressed in both brain areas (Supplementary Table 1). Using RT-qPCR and specific primers to (in)validate our microarray findings, we determined that *Olfr544* transcript is overexpressed at M9 in 5xFAD animals, both in the cortex and the hippocampus (Fig. 1). Eight dysregulated genes in the cortex (*Olfr173*, *Olfr446*, *Olfr544*, *Olfr574*, *Olfr868*, *Olfr1133*, *Olfr1466*, and *Olfr1500*) and seven in the hippocampus (*Olfr446*, *Olfr544*, *Olfr574*, *Olfr868*, *Olfr1133*, *Olfr1466*, and *Olfr1500*) were compared at M4, M6, and M9. We confirmed (i) an under-expression of *Olfr173* in the cortex of transgenic mice, at M4 but not at M6 (Fig. 1a) and *Olfr574* in the cortex at M9 but not in the hippocampus at M6, and (ii) an overexpression of *Olfr868* in the hippocampus at M4 and M6 and *Ollfr1133 i*n the cortex at M9 but not in the hippocampus at M4. Only the overexpression of *Olfr544* is confirmed in both the cortex and hippocampus at M9 (Fig. 1a, b). Interestingly, two OR closely related genes—*Gαolf* and *adenylyl cyclase 3*—are misexpressed in the cortex of 5xFAD mice, at M9 (Supplementary Table 1).

Tissue-Dependent Expression of mRNAs Encoding for Olfr110/111 and Olfr544

We quantified *Olfr110/111*, *Olfr544*, and *Gαolf* gene expression using RT-qPCR in the olfactory mucosa, brain (hippocampus, cortex, and cerebellum), and eyes of WT mice, at M4, M6, M9, and M12. As expected, both OR genes are expressed in the olfactory mucosa of WT and 5xFAD mice (Fig. 2a–c). However, whatever the age considered, *Olfr110/111* is more strongly expressed than *Olfr544* (**$p < 0.01$) (Fig. 2a). We then individually compared brain and eye expressions to those in the olfactory mucosa, used as a reference, in the M6 WT group. The following fold change values are obtained for *Olfr110/111*: − 72 ± 9 (cortex), − 167 ± 35 (hippocampus), − 273 ± 3 (cerebellum), and − 99 ± 18 (eyes) (Fig. 2b). Similar results are observed in M9 and M12 groups. However, at M4, *Olfr110/111* mRNA expression is predominant in the cerebellum (Supplementary Fig. 1a). Similarly, fold change values obtained for *Olfr544* are − 10 ± 2 (cortex), − 7 ± 1 (hippocampus), − 4 ± 1 (cerebellum), and − 9 ± 2 (eyes) (Fig. 2c). *Olfr544* mRNA cerebellar expression is the highest in all age groups (Supplementary Fig. 1b).

Identification of Olfr110/111 and Olfr544 in HEK-Transfected Cells and Olfactory Epithelium

We first examined whether commercial OR antibodies selectively recognize the appropriate OR with immunofluorescence detection, using specific OR-transfected HEK cells (HEK-110, HEK-544) and olfactory mucosa sections as positive controls (Fig. 3). The cells transiently transfected with individual OR genes, tagged with a Flag-epitope at the N-terminus, were stained with both an anti-Flag antibody and commercially available anti-OR antibodies. The rabbit anti-Olfr110/111 and anti-Olfr544 antibodies specifically recognize their corresponding ORs, and these signals co-localize with the Flag epitopes (Fig. 3a–c, e–g). Anti-OR antibodies also detect appropriate olfactory receptor neurons with their distinct dendritic knobs, dendrites, and cell bodies (Fig. 3d, h). Altogether, these results demonstrate the selectivity of the commercial anti-Olfr110/111 and anti-Olfr544 antibodies.

Olfr110/111 and Olfr544 Proteins Are Mainly Expressed in Neurons

Immunohistology reveals the expression of Olfr110/111 and Olfr544 in the cortex and hippocampus of WT (Supplementary Figs. 2 and 3) and transgenic mice (Figs. 4 and 5, Supplementary

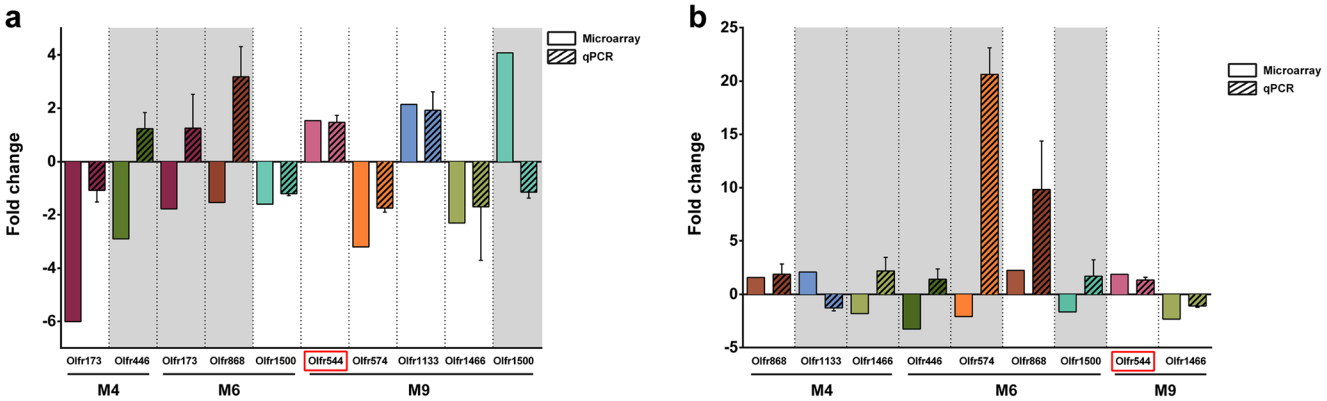

Fig. 1 The cortex (**a**) and hippocampus (**b**) of 5xFAD mice display an extensive dysregulated expression of transcripts coding for olfactory receptors. As shown on supplementary Table 1, microarray analysis indicates that 164 OR mRNAs are over-/under-expressed. Only ten—*Olfr446*, *Olfr538*, *Olfr544*, *Olfr574*, *Olfr720*, *Olfr868*, *Olfr1133*, *Olfr1335*, *Olfr1466*, and *Olfr1500*—are misexpressed in both brain areas. Concordant and discordant results are observed when microarray data are compared to qPCR data. Among the validated dysregulated transcripts, *Olfr544* stands out as a gene which is overexpressed at the same time point, in both the hippocampus and the cortex of transgenic mice

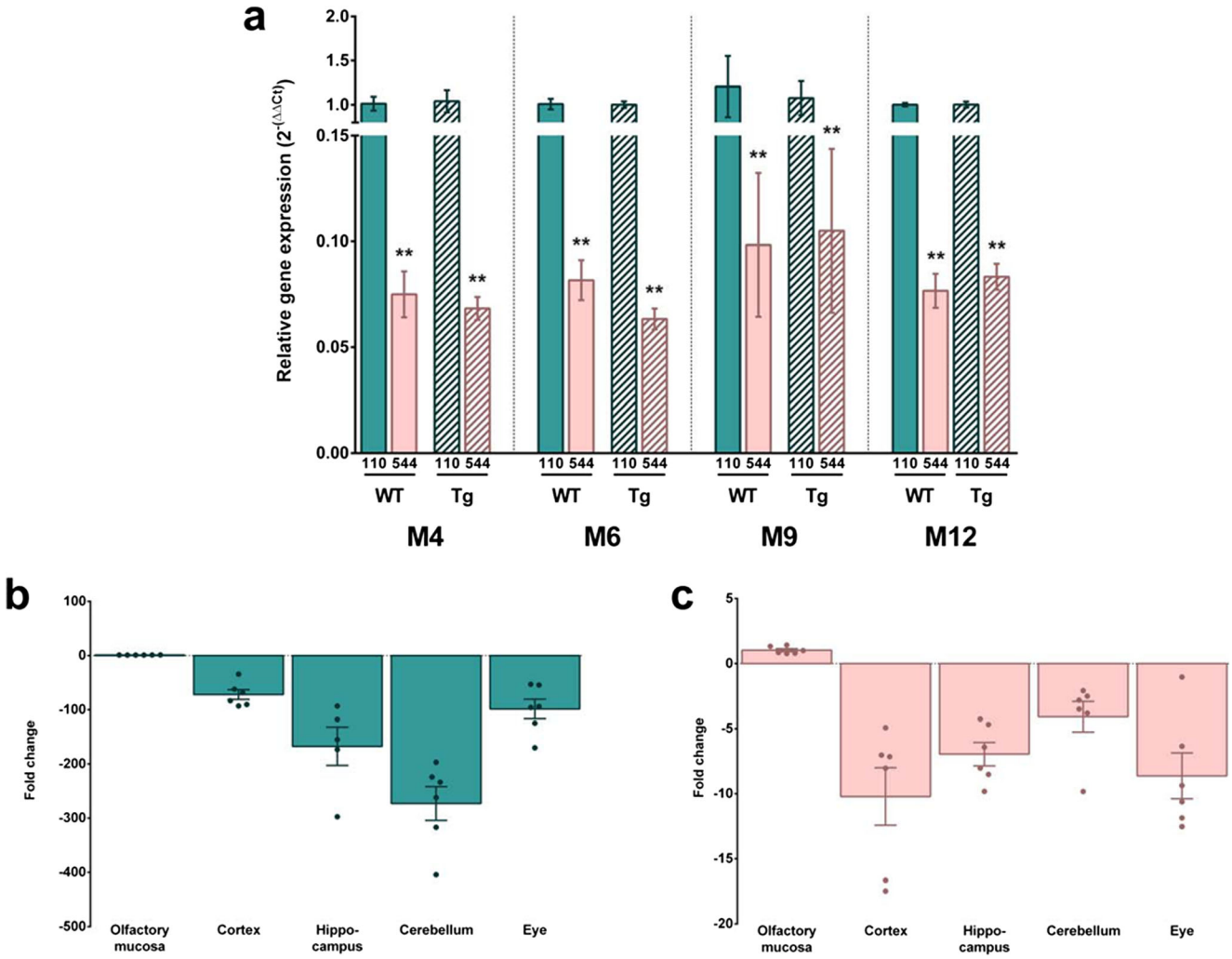

Fig. 2 Tissue- and time-dependent expression of mRNAs encoding for Olfr110/111 and Olfr544. **a** Within the olfactory mucosa, expression of *Olfr110/111* and *Olfr544* mRNA remains stable over time, in both strains. However, the transcript coding for Olfr544 is found in smaller quantities than *Olfr110/111*, at every time point. **b**, **c** In comparison with the olfactory mucosa, *Olfr110/111* and *Olfr544* mRNAs are poorly expressed in the central nervous system. A receptor-related expression profile is observed: *Olfr110/111* is more predominant in the cortex and the eye (**b**) and *Olfr544* in the cerebellum (**c**). $n = 6$ per group. $^{**}p < 0.01$ (Mann and Whitney non-parametric test). M4 4 months, M6 6 months, M9 9 months, M12 12 months, Tg 5xFAD transgenic mice (striped), WT wild-type mice (plain), Olfr110/111 and 110 olfactory receptors 110/111 (green), Olfr544 and 544 olfactory receptor 544 (pink)

Fig. 4). To determine which cell type express those ORs, we double immunostained the sections with neuron-, astrocyte-, oligodendrocyte-, microglia-, and endothelial-specific antibodies.

Neurons Olfr110/111 and Olfr544 are expressed in cortical and hippocampal neurons of M9 5xFAD mice (Fig. 4). More specifically, both OR proteins are mostly produced by neurons in the cortical layers V-VI and, to a lesser extent, in the superficial cortical layers. Within the hippocampus, the most prominent staining is observed in the CA1, CA3 layers, the hilus of the dentate gyrus, and, more faintly, in the dentate gyrus. Both Olfr110/111 and Olfr544 are weakly expressed in a few cortical and hippocampal neurons of M9 WT mice (Supplementary Fig. 2).

Astrocytes Olfr110/111 and Olfr544 are weakly expressed in a few cortical and hippocampal astrocytes of M9 WT mice (Supplementary Fig. 3). In addition, in 5xFAD animals, a faint staining is observed in cortical and hippocampal astrocytes, at M4 and M6, while a stronger labeling is noticed in a few intermediate filaments in M9 animals (Fig. 5a).

Oligodendrocytes A discrete staining of Olfr110/111 is observed in a few oligodendrocyte filaments in the CA1 *stratum oriens* of M9 5xFAD mice. At the same age, in the same animal, no staining of Olfr544 is observed (Fig. 5b).

Microglia Olfr110/111 and Olfr544 are mainly expressed in the cell bodies and proximal segments of microglia, in the

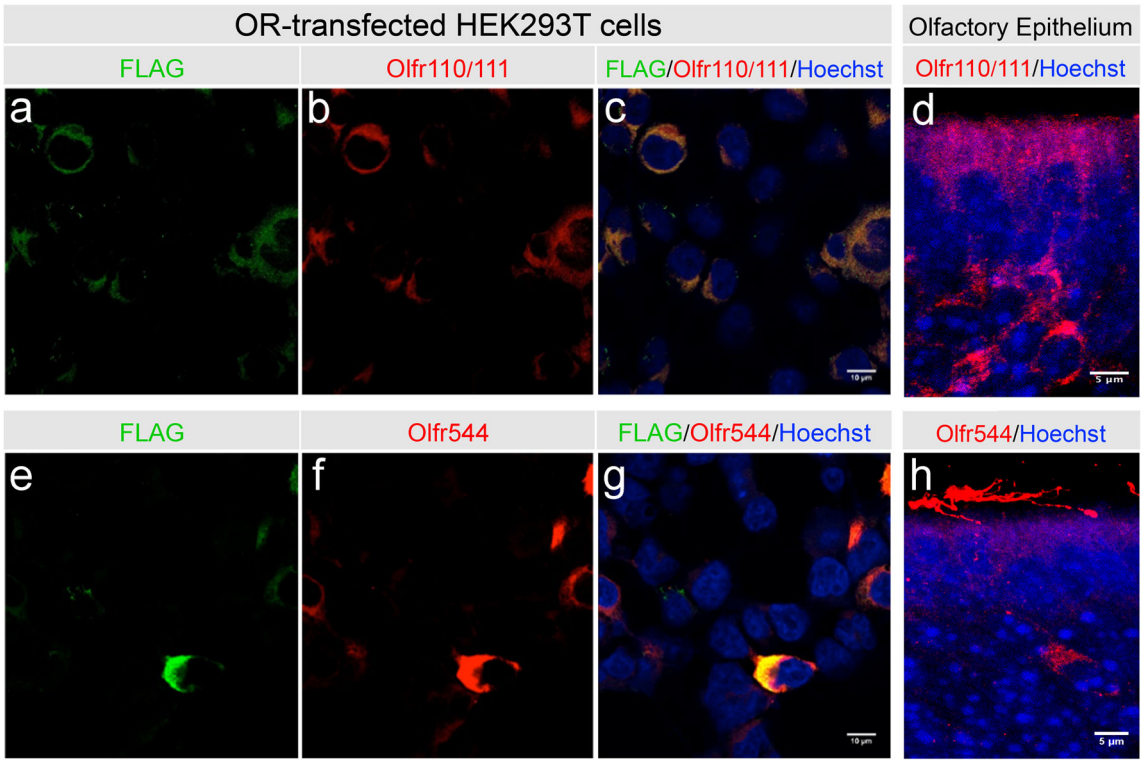

Fig. 3 Validation of commercial antibodies raised against the two olfactory receptors (OR). A heterologous OR expression system in a cell line and the endogenous OR expression in the olfactory epithelium (OE) were used. HEK 293T cells were transiently transfected with cDNAs coding for Olfr110, Olfr544, and immuno-labeled using antibodies against the N-terminal epitope-Flag (**a**, **e**) and each OR-specific antibody (**b**, **f**). Olfr110 (**b**) and Olfr544 (**f**) antibody detect Flag-Olfr110 and Flag-Olfr544-constructs in the transfected cells, respectively. These results are confirmed using the anti-Flag antibody (**a**, **e** and **c**, **g** for overlay). Both OR antibodies recognize specific olfactory receptor neurons (**d**, **h**) in the olfactory epithelium (OE). Scale bar = 10 μm

CA1 *stratum oriens* within the hippocampus of M9 5xFAD mice (Fig. 5c).

Endothelial Cells Olfr110/111 and Olfr544 are observed in the hippocampal CA3 *stratum radiatum* of M9 5xFAD mice. The receptors are localized in the lateral compartments, in close proximity to the lumen, on one side, and the nervous parenchyma, on the other side (Fig. 5d).

With the two ORs being overexpressed in the brain of Alzheimer-like mice, we wondered whether they are associated with β-amyloid plaques. Then, we demonstrated that Olfr110/111 and Olfr544 are expressed in cells located nearby amyloid plaques, especially in the hippocampal CA1 *stratum oriens* (Supplementary Fig. 5).

The Two ORs Are Expressed at the Membrane and in Cells Producing Gαolf

In order to make certain that olfactory receptors are inserted in the cell membrane, we used Alexa488-conjugated wheat germ agglutinin (WGA), a specific membrane marker. We observed a co-localization of Olfr110/111 and Olfr544 with WGA, in the hippocampal CA1 pyramidal layer of M6 WT mice (Fig. 6a, b). Similar results are observed in other hippocampal areas and in cortical layers (Supplementary Fig. 6).

To further determine the potential functionality of the ORs, we investigated whether the olfactory-related protein Gαolf is also expressed in the brain. Gαolf is co-expressed with Olfr110/111 or Olfr544, in the pyramidal layer of CA1 of M9 5xFAD mice (Fig. 6c, d). A similar pattern is also noticed in the dentate gyrus, *cornu ammonis* fields, and in the cortical layers (Supplementary Fig. 7).

Time-Dependent Expression of mRNA Encoding for Olfr110/111 and Olfr544

To assess the kinetic expression of the two ORs of interest, we used transcript expression values at M4, as a reference (Fig. 7). Expression of *Olfr110/111* and *Olfr544* mRNAs varies, according to the age, in the cortex and hippocampus of WT and 5xFAD mice.

Cortical *Olfr110/111* In WT animals ($n = 6$), the fold changes, at M6, M9, and M12, are 1.7 ± 0.3, 2.6 ± 0.5 ($^{*}p < 0.05$), and 6.5 ± 0.9 ($^{**}p < 0.01$), respectively. In transgenic mice ($n = 6$), the fold changes are 7.4 ± 3.1 ($^{**}p < 0.01$), 12 ± 1.8 ($^{**}p < 0.01$), and 28.8 ± 4.4 ($^{**}p < 0.01$), respectively (Fig. 7a).

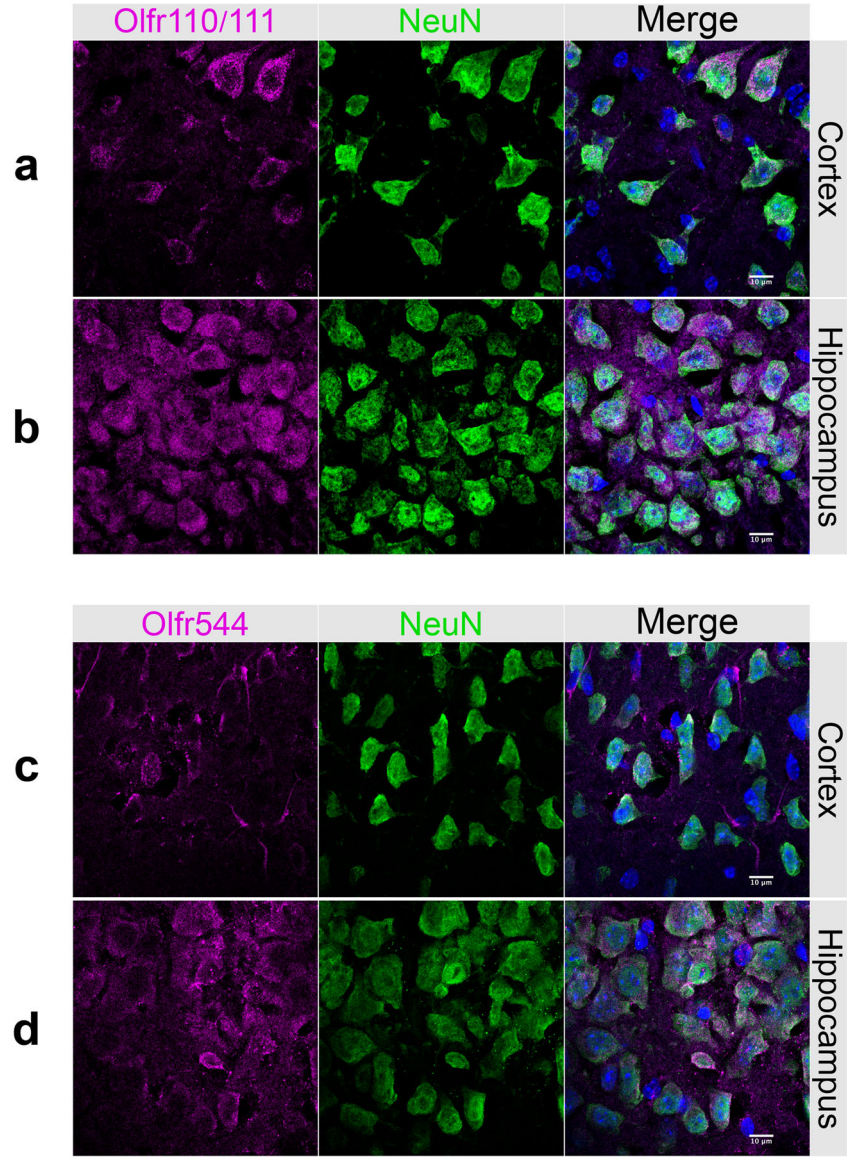

Fig. 4 Neuronal expression of Olfr110/111 and Olfr544. The cortex and hippocampus of M9 transgenic mice were double-immunostained with specific antibodies for neurons (NeuN, green) and the two studied receptors (magenta). Olfr110/111 is expressed by numerous neurons (**a**, **b**), while Olfr544 is produced by a smaller number of neurons (**c**, **d**). Scale bar = 10 μm

Hippocampal *Olfr110/111* In WT animals, the fold changes are 0.8 ± 0.1 ($n = 5$), 0.8 ± 0.1 ($n = 6$), and 2.1 ± 0.3 ($^*p < 0.05$, $n = 6$), respectively. In 5xFAD animals ($n = 6$), the fold changes are 1.7 ± 0.5, 5 ± 1.2 ($^{**}p < 0.01$), and 7 ± 1.8 ($^{**}p < 0.01$), respectively (Fig. 7b).

Cortical *Olfr544* In WT mice ($n = 6$), the fold changes are 1.1 ± 0.2, 1.8 ± 0.2 ($^{**}p < 0.01$), and 1.5 ± 0.2, respectively. In 5xFAD mice ($n = 6$), the fold changes are 1.6 ± 0.3, 1.9 ± 0.3 ($^*p < 0.05$), and 1.5 ± 0.2 (Fig. 7c).

Hippocampal *Olfr544* In WT animals ($n = 6$), the fold changes are 1.4 ± 0.2, 0.9 ± 0.2, and 1.2 ± 0.2, respectively. In transgenic mice, the fold changes are 0.7 ± 0.1 ($n = 5$), 1.3 ± 0.2 ($n = 6$), and 1.5 ± 0.3 ($n = 6$) (Fig. 7d).

A comparison between WT and 5xFAD groups reveals significant changes in the expression of the two ORs in transgenic mice (Supplementary Fig. 8). *Olfr110/111* mRNA is significantly overexpressed in the cortex and hippocampus, whatever the age (Supplementary Fig. 8a-b). Conversely, *Olfr544* transcript expression is unchanged in the hippocampus and slightly increased in the cortex, at M6 (Supplementary Fig. 8c-d).

Gαolf Is Overexpressed in the Cortex at M12

In the olfactory epithelium, olfactory receptors are associated with a specific G-protein named Gαolf. To assess the putative functionality of the brain ORs, we compared *Gαolf* expression in brain areas, using data in the olfactory mucosa as a reference. In WT mice, at M6, the fold changes are − 45 ± 9 (cortex), − 63 ± 16 (hippocampus), − 19 ± 0.7 (cerebellum), and − 327 ± 26 (eyes) (Fig. 8a). From M4 to M12, the same

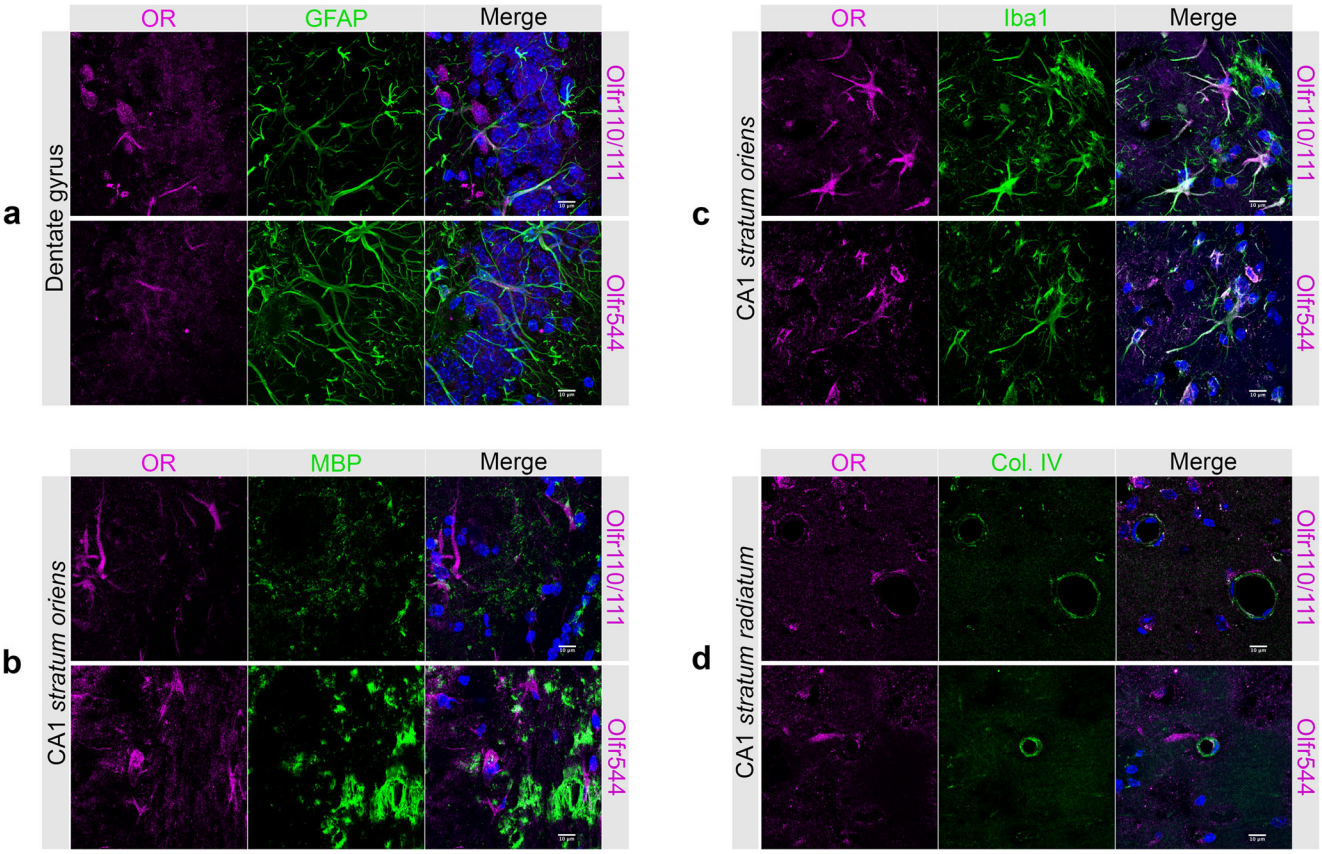

Fig. 5 Expression of Olfr110/111 and Olfr544 in astrocytes, oligodendrocytes, microglia, and endothelial cells. Brain sections of M9 transgenic mice were double-immunostained with specific antibodies for Olfr110/111 or Olfr544 (magenta), astrocytes (**a**), oligodendrocytes (**b**), and microglia (**c**) and endothelial cells (**d**). Olfr110/111 is expressed by all cell types but more predominantly by astrocytes and microglia. All cell types except oligodendrocytes express Olfr544. Scale bar = 10 μm

expression pattern is observed despite varying fold changes (Supplementary Fig. 1c).

Using transcript values at M4, we compared the kinetic expression of *Gαolf* in the cortex and hippocampus of both strains, at M6, M9, and M12.

Cortical *Gaolf* In WT animals ($n = 6$), the fold changes are 0.7 ± 0.2, 0.9 ± 0.1, and 2.6 ± 0.1 (**$p < 0.01$), respectively. In transgenic mice, the fold changes are 1 ± 0.2, 0.7 ± 0.02 (**$p < 0.01$), and 2.3 ± 0.1 (**$p < 0.01$), respectively (Fig. 8b).

Hippocampal *Gaolf* In WT animals, the fold changes are 0.5 ± 0.1 (*$p < 0.05$, $n = 5$), 0.8 ± 0.2 ($n = 5$), and 1.2 ± 0.2 ($n = 6$), respectively. In 5xFAD mice ($n = 6$), the fold changes are 0.8 ± 0.1, 1 ± 0.2, and 1.6 ± 0.5, respectively (Fig. 8c).

Discussion

For the very first time, the current study describes extensively the expression and location of two murine olfactory receptors (ORs) within two brain areas, namely the hippocampus and the adjacent somatosensory cortex. We observed that Olfr110/111 and Olfr544 are (i) mainly produced by neurons, (ii) located in the cytoplasm and the cell membrane, and (iii) associated with one of their usual olfactory partners, Gαolf. Their expression varies throughout the animal's life, whether it is a wild-type or Alzheimer's-like mouse (Fig. 9). In addition, the Olfr110/111- and Olfr544-expressing cells are found nearby amyloid plaques, suggesting a potential role in inflammation.

An Olfactory Machinery in a Non-olfactory Nervous Tissue

The quality and specificity of many antibodies are often problematic. In order to assess the reliability of the selected antibodies for the two ORs of interest, we performed a Western blot using cell lines engineered to produce Olfr110/111 or Olfr544. Reassuringly, we observed the right band at the right molecular weight for both receptors (Supplementary Fig. 9). A first set of immunostaining experiments revealed a punctuated and sometimes clustered cellular staining, exhibiting high similarities with those reported in previous studies [37, 38, 43].

As demonstrated by our dual WGA/Olfr immunostaining experiments, the two olfactory ORs are detected in the cell

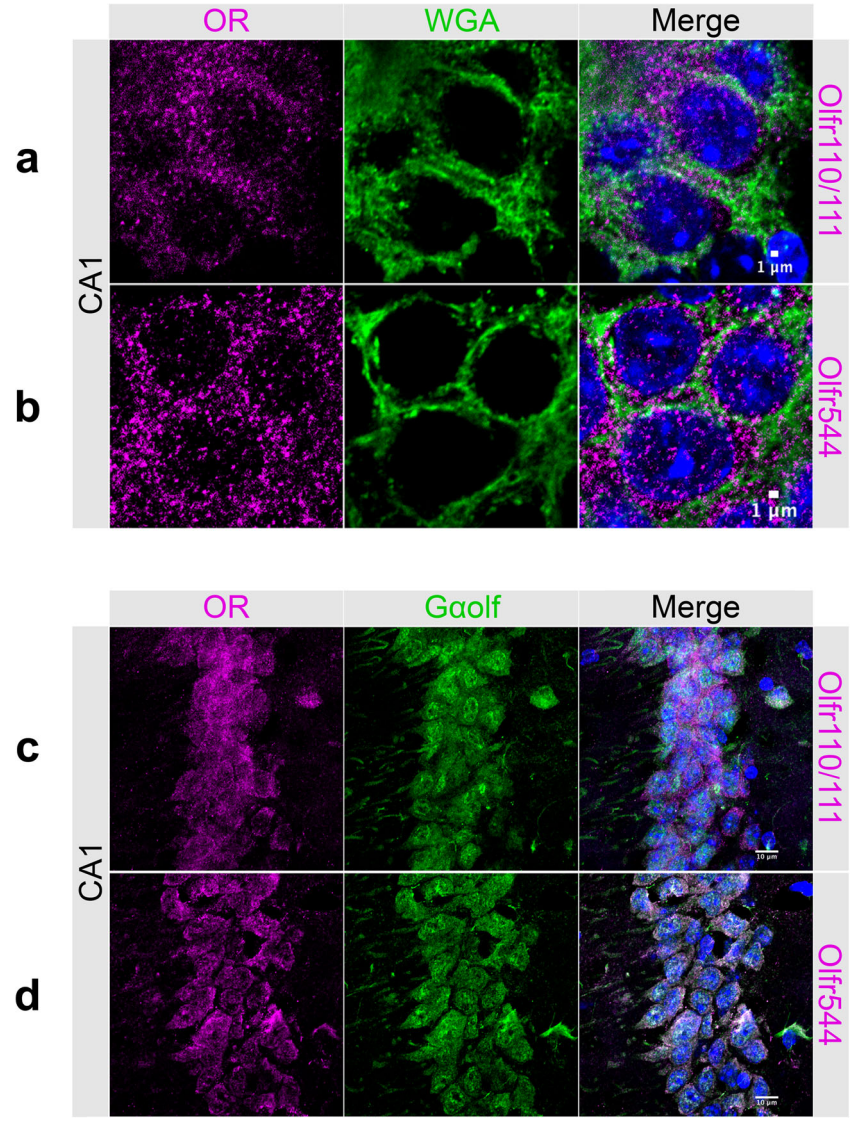

Fig. 6 Olfr110/111 and Olfr544 are present at the cell membrane and co-expressed with Gαolf. Hippocampal sections of a M6 wild-type mouse (**a**) and M9 transgenic mouse (**b**) were double-immunostained with specific antibodies for olfactory receptors (magenta) (**a**–**d**) and Gαolf (green) (**c**, **d**). For the staining of the cell membrane, the fluorescent WGA marker (**a**, **b**) was used. Both receptors are observed at the membrane (**a**, **b**) and are co-expressed with Gαolf (**c**, **d**). Scale bar = 1 μm (**a**) or 10 μm (**b**)

membrane. To further demonstrate their potential functionality, we assessed their co-expression with an olfaction-associated molecule, the Gαolf protein. In the olfactory system, ORs are coupled with Gαolf protein [44], required for transducing an intracellular response after activation of the receptor by a ligand. Previous studies indicated that the mRNA encoding for the Gαolf protein is present in nervous—cortex, basal ganglia, cerebellum, and eyes [36–38, 45–50]—and non-nervous—lungs, kidney, and pancreas [17, 22, 23]—tissues. We confirm here a combined Olfr/Gαolf expression in the cortex and hippocampus of wild-type and transgenic mice. Such a finding suggests a true functionality of the cerebral ORs. However, this does not preclude the possibility that a non-canonical pathway mediates Olfr110/111 and Olfr544 signaling in the brain. For example, OR52B1 signaling is mediated by a Gβγ-protein complex and involves the synthesis of inositol phosphate and diacylglycerol in HCT116 cells [51]. A similar kinetic hippocampal expression of *Gαolf* is observed in both strains. However, transgenic mice display a decreased cortical expression of *Gαolf* at M9. This finding may reflect a global diminution of several receptors, including ORs and others—adenosine A2a receptor, dopamine D1 receptor, and adrenergic β2 receptor—which are known to be associated with Gαolf in the striatum [52–54].

A Preferential Neuronal Expression

In their seminal article, Buck and Axel reported that, within the nervous system, olfactory receptors (ORs) were exclusively expressed in the nasal cavity [1]. Their statement was based on Northern blot experiments, a technique less sensitive than those devised afterward, but it is now well established that ectopic ORs are expressed within the rodent and human central nervous system [32–38]. Using the qPCR technique, we compared *Olfr110/111* and *Olfr544* mRNA production in four

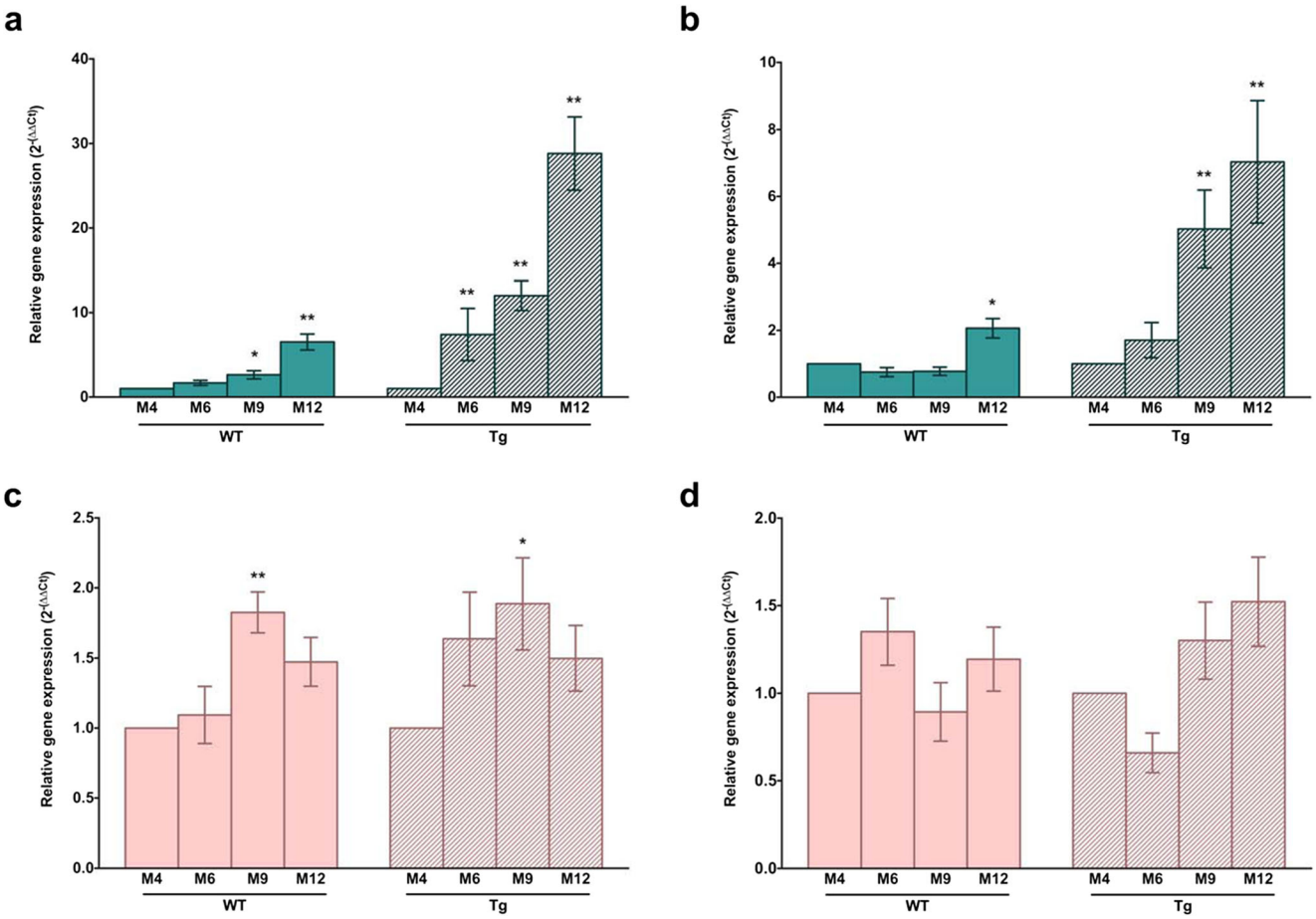

Fig. 7 Time-dependent expression of the transcripts coding for Olfr110/111 (**a**, **b**) and Olfr544 (**c**, **d**) in the cortex and hippocampus of WT and 5xFAD mice. In both the cortex and hippocampus of wild-type and transgenic mice, *Olfr110/111* expression tends to increase with age (**a**, **b**) and the variation reaches statistical significance at M9 and M12. A different profile is noticed for *Olfr544* (**c**, **d**). Overexpression is observed only at M9 in the cortex of both strains. $n = 6$ per group. $^{*}p < 0.05$; $^{**}p < 0.01$ (Mann and Whitney non-parametric test). M4 4 months, M6 6 months, M9 9 months, M12 12 months, Tg 5xFAD transgenic mice (striped), WT wild-type mice (plain), Olfr110/111 olfactory receptors 110/111 (green), Olfr544 olfactory receptor 544 (pink)

brain areas—cerebellum, cortex, hippocampus, and eyeballs—from M6 mice. The latter tissue was selected because the expression of multiple ORs in the mature human retina was recently reported [50]. Both receptors are relatively poorly expressed when each nervous region is compared to the reference tissue, namely the olfactory mucosa, although *Olfr544* is more prevalent than *Olfr110/111*. In addition, each receptor displays a specific pattern: *Olfr110/111* is predominantly expressed in the cortex and the eye, while *Olfr544* is highly produced by the cerebellum.

The brain includes five main cell families: astrocytes, endothelial cells, microglia, neurons, and oligodendrocytes. Using a specific antibody for each cell type, we drew a category map for the hippocampus and the cortex. We observed that Olfr110/111 and Olfr544 are strongly expressed by neurons in both areas, according to the documented expression within the referential tissue, the olfactory neuroepithelium [55, 56], and other nervous tissues [15, 33, 37, 38, 57]. However, ORs are not exclusively found in neurons. Olfr110/111 and Olfr544 are, less abundantly, produced by some astrocytes and microglial cells, as already observed for some OR-expressing glial cells in several areas of the human brain [37]. Olfr110/111 is faintly expressed by a few oligodendrocytes and endothelial cells, whereas Olfr544 is only observed in endothelial cells.

An Age- and Pathology-Dependent Expression

Within the olfactory mucosa, *Olfr110/111* transcript is more strongly expressed than *Olfr544*. However, their production remains steady, whatever the age considered. Conversely, the kinetic expression of both ORs indicates an age-related dysregulation in wild-type animals.

As an example, we observed an increased expression of *Olfr110/111* mRNA in the cortex, at M9 and M12, and in the hippocampus, at M12. These results are discordant with a study reporting no age-related modified expression for *Olfr110/111* within the cortex. Nevertheless, this could be

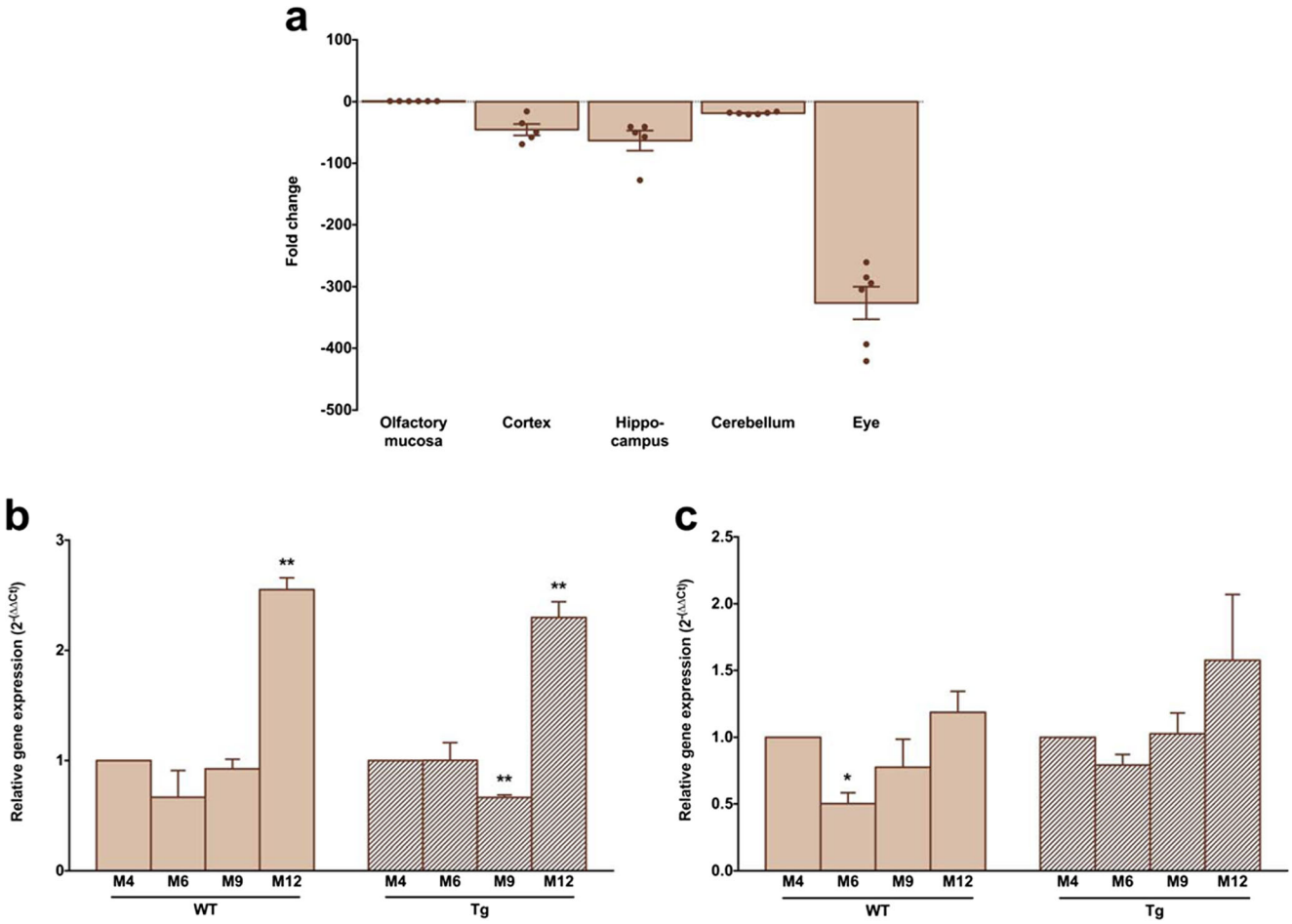

Fig. 8 Tissue- and time-dependent expression of the mRNA coding for Gαolf. In comparison with the olfactory mucosa, *Gαolf* is poorly expressed in the eyes and, to a lesser extent, in the other examined brain areas (**a**). Within the cortex, *Gαolf* is overexpressed at M12 in both strains (**b**), while, in the hippocampus of wild-type mice, it is under-expressed at M6 (**c**). $n = 6$ per group. $^{*}p < 0.05$; $^{**}p < 0.01$ (Mann and Whitney non-parametric test). M4 4 months, M6 6 months, M9 9 months, M12 12 months, Tg 5xFAD transgenic mice (striped), WT wild-type mice (plain)

related to sexual dimorphism, since the previous observations were made in female mice [36].

A dysregulated expression of human OR genes has been found in several neuropathologies such as Parkinson's disease [37], Alzheimer's disease (AD), progressive supranuclear palsy, Creutzfeldt-Jakob disease [36], and schizophrenia [39]. We show here that AD pathology does not affect the nasal expression of the two ORs of interest. On the contrary, the production of numerous ORs transcripts is dysregulated in the cortex and hippocampus of transgenic mice modeling AD. These results are partially in line with findings reported in the human entorhinal and frontal cortices: six OR genes are either under- or overexpressed, depending on the stage of the disease [36]. In addition, the current study demonstrates that the expression of many OR transcripts also varies in the hippocampus, in line with AD symptomatology.

In a study based on APP/PS1 transgenic mice, another model of AD, it was shown that *Olfr110* expression increases from birth to M12 [36]. Similarly, a transcriptomic experiment on 5xFAD mice reported a hippocampal overexpression of *Olfr110* [58]. In line with these previous studies, we show here that transgenic 5xFAD mice exhibit an enhanced expression of *Olfr110/111* in the cortex, from M6 to M12, and in the hippocampus, from M9 to M12. Altogether, these results indicate that this OR may play a role in AD pathology. In contrast, the putative role of *Olfr544* is more uncertain since this receptor is only overexpressed at M9 in the cortex of 5xFAD mice.

Fig. 9 Graphical summary. Time-, strain-, and cell type-dependent expression of Olfr110/111 and Olfr544 in the brain. **a** Overall, *Olfr110/111* is more highly expressed in Alzheimer's like mice and its overexpression increases with age. No strain- and age-associated change is observed for *Olfr544*. **b** Olfr110/111 and Olfr544 are mostly expressed by neurons and to a lesser extent by astrocytes, microglia, and endothelial cells. Only Olfr110/111 is expressed by oligodendrocytes, during late adulthood in 5XFAD mice. OR expression level in neural cells is indicated using a red gradient, ranging from the lowest to the highest

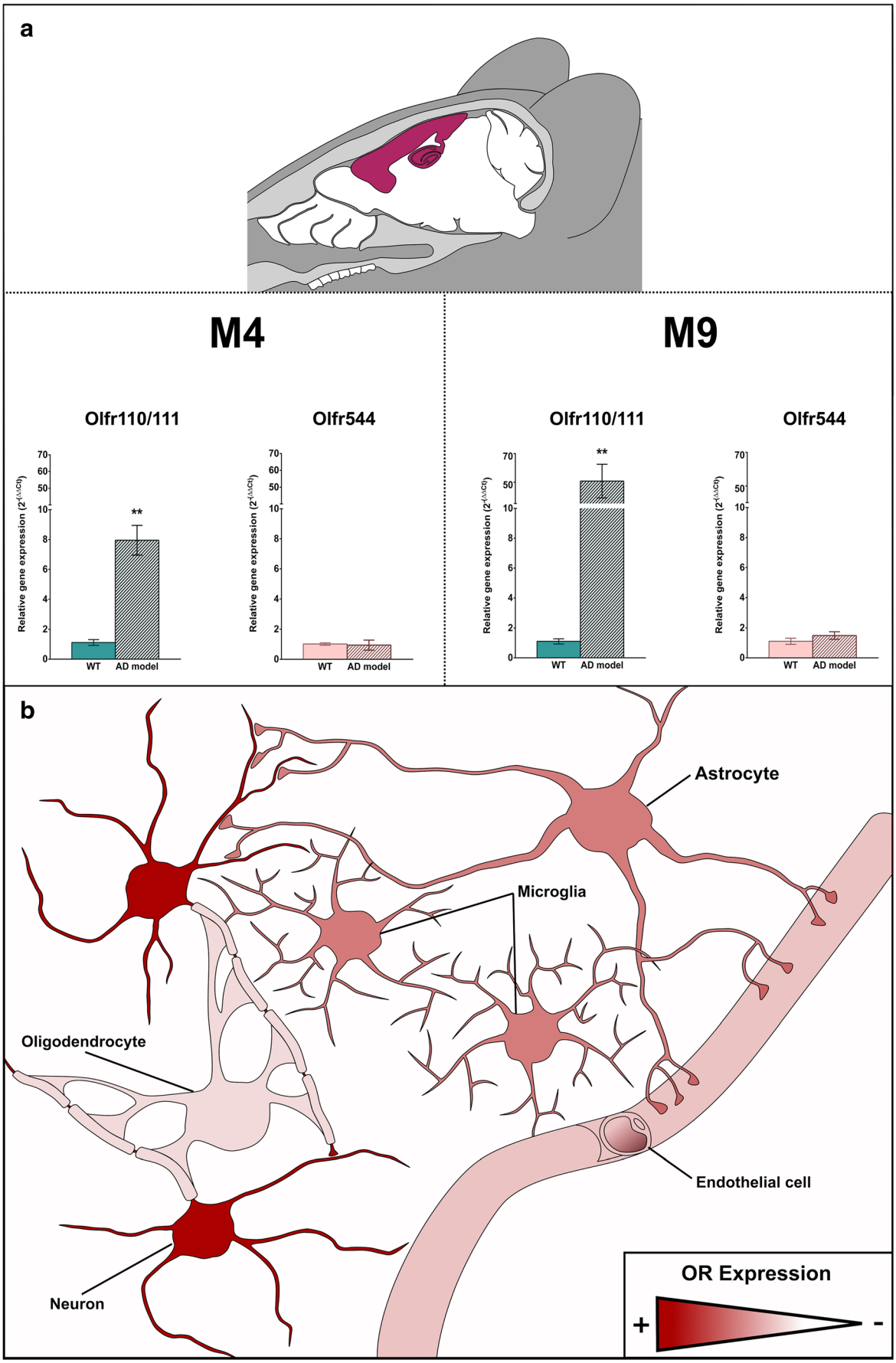
a
M4
M9
Olfr110/111
Olfr544
Olfr110/111
Olfr544
Relative gene expression (2^-ΔΔCt)
**
WT
AD model
b
Astrocyte
Microglia
Oligodendrocyte
Endothelial cell
Neuron
OR Expression
+
-

Possible Role(s) as Immuno-modulators and Mechano-sensors

We report here that the expression of cortical and hippocampal *Olfr110/111*, and cortical *Olfr544* mRNAs is increased in 5xFAD mice during the late stages of the pathology. Moreover, both ORs are detected nearby amyloid plaques in the brains of M9 5xFAD mice. Combined together, our results suggest that Olfr110/111 and Olfr544 are potentially involved in neuroinflammatory processes.

In support of this hypothesis, we can cite a study showing an overexpression of *Olfr110* mRNA in cultivated, lipopolysaccharide-activated microglia from *ApoE* knocked-in mice, a model of tauopathy [59]. A presumed link between both ORs and neuroinflammation is reinforced by data indicating an age-associated development of an inflammatory response in C57Bl/6 mice and in human brains [60–63].

More generally, OR involvement in neuroinflammatory processes is increasingly recognized. The activation of two human ORs (OR1D2 and OR2AG1) expressed in airway smooth muscle cells triggers inflammation and contraction of these cells [17]. Similarly, after a sciatic nerve transection, during a phase associated with the detection of stimuli, a dysregulated expression of several olfactory receptors (e.g., *Olfr40*, *463*, *629*, *728*, *1108*, and *1589*) was observed [64].

Certain ORs are also known to trigger physiological responses without an agonist stimulation. Interestingly, it has been demonstrated that heterologous expression of an OR confers mechanosensitivity to its host cells, indicating that certain ORs are both necessary and sufficient to cause mechanical responses, without any ligand stimulation [65]. Previous studies also report that the expression of G protein-coupled receptors (GPCRs) can affect metabolism of the amyloid protein precursor (APP) [66]. For example, the expression, without stimulation, of serotonin receptor (5-HT4R) induces APP cleavage, independently of cAMP production, as 5-HT4Rs physically interact with the mature form of ADAM10 [67]. This mechanosensitive function of the cerebral ORs may induce physiological responses to several mechanical stimuli (pressure, stress, membrane stretch).

Conclusion

Our study aimed to characterize the expression profiles of two ORs in the murine brain, in physiological conditions and in a neurodegenerative context. We demonstrate for the first time the expression of Olfr110/111 and Olfr544 at the transcript and protein levels, in the cortex and hippocampus, along with Gαolf protein. Olfr110/111 and Olfr544 are mainly expressed not only by hippocampal and cortical neurons but also by astrocytes, microglia, oligodendrocytes, and endothelial cells. Moreover, Olfr110/111 and Olfr544 proteins are present at the cell membrane, likely associated with Gαolf, granting them a potential functionality at the cerebral level. OR mRNA expression is also dysregulated in the 5xFAD transgenic model of AD. The current report represents a new and stimulating insight in the field of neuropathologies, particularly Alzheimer's disease. Further studies are required to shed light on the cerebral roles and implications of Olfr110/111 and Olfr544, with exciting possibilities and potential outcomes for drug development.

Acknowledgements We thank Kevin Baranger for providing the animals needed and for its helpful comments.

Funding Information This work was supported by a research grant from the GPM ("Groupement Pasteur Mutualité"). Fanny Gaudel was a recipient of fellowships from the Edmond Roudnitska Foundation.

Compliance with Ethical Standards

Conflict of Interest The authors declare that they have no competing financial interests.

References

1. Buck L, Axel R (1991) A novel multigene family may encode odorant receptors: a molecular basis for odor recognition. Cell 65: 175–187
2. Parmentier M, Libert F, Schurmans S, Schiffmann S, Lefort A, Eggerickx D, Ledent C, Mollereau C et al (1992) Expression of members of the putative olfactory receptor gene family in mammalian germ cells. Nature 355:453–455. https://doi.org/10.1038/355453a0
3. Asai H, Kasai H, Matsuda Y, Yamazaki N, Nagawa F, Sakano H, Tsuboi A (1996) Genomic structure and transcription of a murine odorant receptor gene: differential initiation of transcription in the olfactory and testicular cells. Biochem Biophys Res Commun 221: 240–247. https://doi.org/10.1006/bbrc.1996.0580
4. Vanderhaeghen P, Schurmans S, Vassart G, Parmentier M (1997) Specific repertoire of olfactory receptor genes in the male germ cells of several mammalian species. Genomics 39:239–246. https://doi.org/10.1006/geno.1996.4490
5. Goto T, Salpekar A, Monk M (2001) Expression of a testis-specific member of the olfactory receptor gene family in human primordial germ cells. Mol Hum Reprod 7:553–558
6. Volz A, Ehlers A, Younger R, Forbes S, Trowsdale J, Schnorr D, Beck S, Ziegler A (2003) Complex transcription and splicing of odorant receptor genes. J Biol Chem 278:19691–19701. https://doi.org/10.1074/jbc.M212424200
7. Fukuda N, Yomogida K, Okabe M, Touhara K (2004) Functional characterization of a mouse testicular olfactory receptor and its role in chemosensing and in regulation of sperm motility. J Cell Sci 117: 5835–5845. https://doi.org/10.1242/jcs.01507
8. Fukuda N, Touhara K (2006) Developmental expression patterns of testicular olfactory receptor genes during mouse spermatogenesis: olfactory receptor expression in mouse germ cells. Genes Cells 11: 71–81. https://doi.org/10.1111/j.1365-2443.2005.00915.x
9. Sanz G, Schlegel C, Pernollet J-C, Briand L (2005) Comparison of odorant specificity of two human olfactory receptors from different phylogenetic classes and evidence for antagonism. Chem Senses 30:69–80. https://doi.org/10.1093/chemse/bji002

10. Saito H, Chi Q, Zhuang H, Matsunami H, Mainland JD (2009) Odor coding by a mammalian receptor repertoire. Sci Signal 2: ra9. https://doi.org/10.1126/scisignal.2000016
11. Veitinger T, Riffell JR, Veitinger S, Nascimento JM, Triller A, Chandsawangbhuwana C, Schwane K, Geerts A et al (2011) Chemosensory Ca2+ dynamics correlate with diverse behavioral phenotypes in human sperm. J Biol Chem 286:17311–17325. https://doi.org/10.1074/jbc.M110.211524
12. Adipietro KA, Mainland JD, Matsunami H (2012) Functional evolution of mammalian odorant receptors. PLoS Genet 8:e1002821. https://doi.org/10.1371/journal.pgen.1002821
13. Walensky LD, Roskams AJ, Lefkowitz RJ, Snyder SH, Ronnett GV (1995) Odorant receptors and desensitization proteins colocalize in mammalian sperm. Mol Med Camb Mass 1:130–141
14. Vanderhaeghen P, Schurmans S, Vassart G, Parmentier M (1997) Molecular cloning and chromosomal mapping of olfactory receptor genes expressed in the male germ line: evidence for their wide distribution in the human genome. Biochem Biophys Res Commun 237:283–287. https://doi.org/10.1006/bbrc.1997.7043
15. Weber M, Pehl U, Breer H, Strotmann J (2002) Olfactory receptor expressed in ganglia of the autonomic nervous system. J Neurosci Res 68:176–184
16. Gu X, Karp PH, Brody SL, Pierce RA, Welsh MJ, Holtzman MJ, Ben-Shahar Y (2014) Chemosensory functions for pulmonary neuroendocrine cells. Am J Respir Cell Mol Biol 50:637–646. https://doi.org/10.1165/rcmb.2013-0199OC
17. Kalbe B, Knobloch J, Schulz VM, Wecker C, Schlimm M, Scholz P, Jansen F, Stoelben E et al (2016) Olfactory receptors modulate physiological processes in human airway smooth muscle cells. Front Physiol 7:339. https://doi.org/10.3389/fphys.2016.00339
18. Busse D, Kudella P, Grüning N-M, Gisselmann G, Ständer S, Luger T, Jacobsen F, Steinsträßer L et al (2014) A synthetic sandalwood odorant induces wound-healing processes in human keratinocytes via the olfactory receptor OR2AT4. J Investig Dermatol 134:2823–2832. https://doi.org/10.1038/jid.2014.273
19. Gelis L, Jovancevic N, Veitinger S, Mandal B, Arndt HD, Neuhaus EM, Hatt H (2016) Functional characterization of the odorant receptor 51E2 in human melanocytes. J Biol Chem 291:17772–17786. https://doi.org/10.1074/jbc.M116.734517
20. Tsai T, Veitinger S, Peek I, Busse D, Eckardt J, Vladimirova D, Jovancevic N, Wojcik S et al (2016) Two olfactory receptors -OR2A4/7 and OR51B5- differentially affect epidermal proliferation and differentiation. Exp Dermatol 26:58–65. https://doi.org/10.1111/exd.13132
21. Zhang X, De la Cruz O, Pinto JM et al (2007) Characterizing the expression of the human olfactory receptor gene family using a novel DNA microarray. Genome Biol 8:R86. https://doi.org/10.1186/gb-2007-8-5-r86
22. Pluznick JL, Zou D-J, Zhang X, Yan Q, Rodriguez-Gil DJ, Eisner C, Wells E, Greer CA et al (2009) Functional expression of the olfactory signaling system in the kidney. Proc Natl Acad Sci U S A 106:2059–2064. https://doi.org/10.1073/pnas.0812859106
23. Kang N, Bahk YY, Lee N, Jae YG, Cho YH, Ku CR, Byun Y, Lee EJ et al (2015) Olfactory receptor Olfr544 responding to azelaic acid regulates glucagon secretion in α-cells of mouse pancreatic islets. Biochem Biophys Res Commun 460:616–621. https://doi.org/10.1016/j.bbrc.2015.03.078
24. Feldmesser E, Olender T, Khen M, Yanai I, Ophir R, Lancet D (2006) Widespread ectopic expression of olfactory receptor genes. BMC Genomics 7:121. https://doi.org/10.1186/1471-2164-7-121
25. Kang N, Koo J (2012) Olfactory receptors in non-chemosensory tissues. BMB Rep 45:612–622
26. Flegel C, Manteniotis S, Osthold S, Hatt H, Gisselmann G (2013) Expression profile of ectopic olfactory receptors determined by deep sequencing. PLoS One 8:e55368. https://doi.org/10.1371/journal.pone.0055368
27. Flegel C, Schöbel N, Altmüller J, Becker C, Tannapfel A, Hatt H, Gisselmann G (2015) RNA-Seq analysis of human trigeminal and dorsal root ganglia with a focus on chemoreceptors. PLoS One 10: e0128951. https://doi.org/10.1371/journal.pone.0128951
28. Griffin CA, Kafadar KA, Pavlath GK (2009) MOR23 promotes muscle regeneration and regulates cell adhesion and migration. Dev Cell 17:649–661. https://doi.org/10.1016/j.devcel.2009.09.004
29. Braun T, Voland P, Kunz L, Prinz C, Gratzl M (2007) Enterochromaffin cells of the human gut: sensors for spices and odorants. Gastroenterology 132:1890–1901. https://doi.org/10.1053/j.gastro.2007.02.036
30. Pluznick JL, Protzko RJ, Gevorgyan H, Peterlin Z, Sipos A, Han J, Brunet I, Wan LX et al (2013) Olfactory receptor responding to gut microbiota-derived signals plays a role in renin secretion and blood pressure regulation. Proc Natl Acad Sci U S A 110:4410–4415. https://doi.org/10.1073/pnas.1215927110
31. Spehr M (2003) Identification of a testicular odorant receptor mediating human sperm chemotaxis. Science 299:2054–2058. https://doi.org/10.1126/science.1080376
32. Raming K, Konzelmann S, Breer H (1998) Identification of a novel G-protein coupled receptor expressed in distinct brain regions and a defined olfactory zone. Recept Channels 6:141–151
33. Conzelmann S, Levai O, Bode B, Eisel U, Raming K, Breer H, Strotmann J (2000) A novel brain receptor is expressed in a distinct population of olfactory sensory neurons. Eur J Neurosci 12:3926–3934
34. Yuan TT, Toy P, McClary JA et al (2001) Cloning and genetic characterization of an evolutionarily conserved human olfactory receptor that is differentially expressed across species. Gene 278: 41–51
35. Otaki JM, Yamamoto H, Firestein S (2004) Odorant receptor expression in the mouse cerebral cortex. J Neurobiol 58:315–327. https://doi.org/10.1002/neu.10272
36. Ansoleaga B, Garcia-Esparcia P, Llorens F, Moreno J, Aso E, Ferrer I (2013) Dysregulation of brain olfactory and taste receptors in AD, PSP and CJD, and AD-related model. Neuroscience 248:369–382. https://doi.org/10.1016/j.neuroscience.2013.06.034
37. Garcia-Esparcia P, Schlüter A, Carmona M, Moreno J, Ansoleaga B, Torrejón-Escribano B, Gustincich S, Pujol A et al (2013) Functional genomics reveals dysregulation of cortical olfactory receptors in Parkinson disease: Novel putative chemoreceptors in the human brain. J Neuropathol Exp Neurol 72:524–539. https://doi.org/10.1097/NEN.0b013e318294fd76
38. Grison A, Zucchelli S, Urzì A, Zamparo I, Lazarevic D, Pascarella G, Roncaglia P, Giorgetti A et al (2014) Mesencephalic dopaminergic neurons express a repertoire of olfactory receptors and respond to odorant-like molecules. BMC Genomics 15:729. https://doi.org/10.1186/1471-2164-15-729
39. Ansoleaga B, Garcia-Esparcia P, Pinacho R, Haro JM, Ramos B, Ferrer I (2015) Decrease in olfactory and taste receptor expression in the dorsolateral prefrontal cortex in chronic schizophrenia. J Psychiatr Res 60:109–116. https://doi.org/10.1016/j.jpsychires.2014.09.012
40. Hawrylycz MJ, Lein ES, Guillozet-Bongaarts AL, Shen EH, Ng L, Miller JA, van de Lagemaat LN, Smith KA et al (2012) An anatomically comprehensive atlas of the adult human brain transcriptome. Nature 489:391–399. https://doi.org/10.1038/nature11405
41. Oakley H, Cole SL, Logan S, Maus E, Shao P, Craft J, Guillozet-Bongaarts A, Ohno M et al (2006) Intraneuronal beta-amyloid aggregates, neurodegeneration, and neuron loss in transgenic mice with five familial Alzheimer's disease mutations: potential factors in amyloid plaque formation. J Neurosci 26:10129–10140. https://doi.org/10.1523/JNEUROSCI.1202-06.2006

42. Belloir C, Miller-Leseigneur M-L, Neiers F, Briand L, le Bon AM (2017) Biophysical and functional characterization of the human olfactory receptor OR1A1 expressed in a mammalian inducible cell line. Protein Expr Purif 129:31–43. https://doi.org/10.1016/j.pep.2016.09.006
43. Low VF, Mombaerts P (2017) Odorant receptor proteins in the mouse main olfactory epithelium and olfactory bulb. Neuroscience 344:167–177. https://doi.org/10.1016/j.neuroscience.2016.12.044
44. Jones DT, Reed RR (1989) Golf: an olfactory neuron specific-G protein involved in odorant signal transduction. Science 244:790–795
45. Drinnan SL, Hope BT, Snutch TP, Vincent SR (1991) G(olf) in the basal ganglia. Mol Cell Neurosci 2:66–70
46. Hervé D, Rogard M, Lévi-Strauss M (1995) Molecular analysis of the multiple golf alpha subunit mRNAs in the rat brain. Brain Res Mol Brain Res 32:125–134
47. Belluscio L, Gold GH, Nemes A, Axel R (1998) Mice deficient in G(olf) are anosmic. Neuron 20:69–81
48. Vemula SR, Puschmann A, Xiao J, Zhao Y, Rudzińska M, Frei KP, Truong DD, Wszolek ZK et al (2013) Role of Gα(olf) in familial and sporadic adult-onset primary dystonia. Hum Mol Genet 22:2510–2519. https://doi.org/10.1093/hmg/ddt102
49. Pronin A, Levay K, Velmeshev D, Faghihi M, Shestopalov VI, Slepak VZ (2014) Expression of olfactory signaling genes in the eye. PLoS One 9:e96435. https://doi.org/10.1371/journal.pone.0096435
50. Jovancevic N, Khalfaoui S, Weinrich M, Weidinger D, Simon A, Kalbe B, Kernt M, Kampik A et al (2017) Odorant receptor 51E2 agonist β-ionone regulates RPE cell migration and proliferation. Front Physiol 8. https://doi.org/10.3389/fphys.2017.00888
51. Weber L, Al-Refae K, Ebbert J et al (2017) Activation of odorant receptor in colorectal cancer cells leads to inhibition of cell proliferation and apoptosis. PLoS One 12:e0172491. https://doi.org/10.1371/journal.pone.0172491
52. Hervé D, Le Moine C, Corvol JC et al (2001) Galpha(olf) levels are regulated by receptor usage and control dopamine and adenosine action in the striatum. J Neurosci 21:4390–4399
53. Corvol JC, Studler JM, Schonn JS, Girault JA, Hervé D (2001) Galpha(olf) is necessary for coupling D1 and A2a receptors to adenylyl cyclase in the striatum. J Neurochem 76:1585–1588
54. Hara M, Fukui R, Hieda E, Kuroiwa M, Bateup HS, Kano T, Greengard P, Nishi A (2010) Role of adrenoceptors in the regulation of dopamine/DARPP-32 signaling in neostriatal neurons. J Neurochem 113:1046–1059. https://doi.org/10.1111/j.1471-4159.2010.06668.x
55. Shepherd GM (1985) The olfactory system: the uses of neural space for a non-spatial modality. Prog Clin Biol Res 176:99–114
56. Buck LB (1996) Information coding in the vertebrate olfactory system. Annu Rev Neurosci 19:517–544. https://doi.org/10.1146/annurev.ne.19.030196.002505
57. Gong L, Chen Q, Gu X, Li S (2015) Expression and identification of olfactory receptors in sciatic nerve and dorsal root ganglia of rats. Neurosci Lett 600:171–175. https://doi.org/10.1016/j.neulet.2015.06.019
58. Siwek ME, Müller R, Henseler C, Trog A, Lundt A, Wormuth C, Broich K, Ehninger D et al (2015) Altered theta oscillations and aberrant cortical excitatory activity in the 5XFAD model of Alzheimer's disease. Neural Plast 2015:781731. https://doi.org/10.1155/2015/781731
59. Shi Y, Yamada K, Liddelow SA, Smith ST, Zhao L, Luo W, Tsai RM, Spina S et al (2017) ApoE4 markedly exacerbates tau-mediated neurodegeneration in a mouse model of tauopathy. Nature 549:523–527. https://doi.org/10.1038/nature24016
60. Machado-Salas JP, Scheibel AB (1979) Limbic system of the aged mouse. Exp Neurol 63:347–355
61. Lee CK, Weindruch R, Prolla TA (2000) Gene-expression profile of the ageing brain in mice. Nat Genet 25:294–297. https://doi.org/10.1038/77046
62. Lu T, Pan Y, Kao S-Y, Li C, Kohane I, Chan J, Yankner BA (2004) Gene regulation and DNA damage in the ageing human brain. Nature 429:883–891. https://doi.org/10.1038/nature02661
63. Raj D, Yin Z, Breur M, Doorduin J, Holtman IR, Olah M, Mantingh-Otter IJ, van Dam D et al (2017) Increased white matter inflammation in aging- and Alzheimer's disease brain. Front Mol Neurosci 10:206. https://doi.org/10.3389/fnmol.2017.00206
64. Li S, Liu Q, Wang Y, Gu Y, Liu D, Wang C, Ding G, Chen J et al (2013) Differential gene expression profiling and biological process analysis in proximal nerve segments after sciatic nerve transection. PLoS One 8:e57000. https://doi.org/10.1371/journal.pone.0057000
65. Connelly T, Yu Y, Grosmaitre X, Wang J, Santarelli LC, Savigner A, Qiao X, Wang Z et al (2015) G protein-coupled odorant receptors underlie mechanosensitivity in mammalian olfactory sensory neurons. Proc Natl Acad Sci 112:590–595. https://doi.org/10.1073/pnas.1418515112
66. Thathiah A, De Strooper B (2011) The role of G protein-coupled receptors in the pathology of Alzheimer's disease. Nat Rev Neurosci 12:73–87. https://doi.org/10.1038/nrn2977
67. Cochet M, Donneger R, Cassier E, Gaven F, Lichtenthaler SF, Marin P, Bockaert J, Dumuis A et al (2013) 5-HT4 receptors constitutively promote the non-amyloidogenic pathway of APP cleavage and interact with ADAM10. ACS Chem Neurosci 4:130–140. https://doi.org/10.1021/cn300095t